This article has been accepted for publication in a future issue of this journal, but has not been fully edited. Content may change prior to final publication. Citation information: DOI 10.1109/LCOMM.2020.2981609, IEEE Communications Letters

Channel Characterization for 1D Molecular Communication with Two Absorbing Receivers

Xinyu Huang, *Student Member, IEEE*, Yuting Fang, Adam Noel, *Member, IEEE*, and Nan Yang, *Senior Member, IEEE*

***Abstract*—This letter develops a one-dimensional (1D) diffusion-based molecular communication system to analyze channel responses between a single transmitter (TX) and two fully-absorbing receivers (RXs). Incorporating molecular degradation in the environment, rigorous analytical formulas for i) the fraction of molecules absorbed, ii) the corresponding hitting rate, and iii) the asymptotic fraction of absorbed molecules as time approaches infinity at each RX are derived when an impulse of molecules are released at the TX. By using particle-based simulations, the derived analytical expressions are validated. Simulations also present the distance ranges of two RXs that do not impact molecular absorption of each other, and demonstrate that the mutual influence of two active RXs reduces with the increase in the degradation rate.**

I. Introduction

Molecular communication (MC) is one of the most promising solutions to nano-scale communications. In MC, information is encoded into small particles that are released by a transmitter (TX) into a fluid medium and propagate until they arrive at a receiver (RX). Moreover, MC can be biocompatible and consumes low energy. These characteristics make MC suitable for applications such as targeted drug delivery, pollution control, and environmental monitoring [1]. For each application, accurate channel modeling is essential for analysis and design of MC systems [2].

Most existing MC papers have focused on the modeling of a single-RX MC system [3]. Some papers, e.g., [4]–[7], have considered a multi-RX MC system. The majority of papers involving a multi-RX MC system have assumed transparent RXs for tractability, due to the independence among observations at multiple transparent RXs. However, many practical RX surfaces might interact with the molecules of interest, e.g., by providing binding sites for absorption or other reactions [8]. In an environment where multiple non-transparent RXs co-exist, one non-transparent RX would impact molecules received by other non-transparent RXs. Hence, an accurate characterization of such dependence makes the derivation of channel response (CR) cumbersome. Motivated by this, [5]–[7] have considered a multi-RX system with non-transparent RXs. In [5], the capture probability for each receiver was obtained via simulations. Considering a one-dimensional (1D) environment with two fully-absorbing RXs, [6] derived the sum of absorbed molecules by both RXs. Notably, [7] derived the fraction of molecules absorbed at each RX in a three-dimensional (3D) environment with two fully-absorbing RXs. However, this derivation is not applicable in a 1D environment, as we will show in Section IV. Thus, an exact closed-form expression for the fraction of molecules absorbed over time at each RX (i.e., the CR) has not been derived yet for a 1D environment.

Despite the aforementioned challenges, we provide closed-form expressions for the fraction of molecules absorbed at RXs when multiple fully-absorbing RXs co-exist, by taking into account the mutual influence between RXs. Such expressions accurately characterize the CR at fully-absorbing RXs and lay the foundation for future performance evaluation, detection design, and diverse applications (e.g., target detection using two fully-absorbing RXs) of a realistic multi-RX system. In this letter, we consider a 1D environment where one TX communicates between two fully-absorbing RXs. The 1D environment is worthy of investigation since it is a good first approximation for regions between two close cells, such as chemical synapses in a human body [9]. To capture the effect of molecular chemical reaction on the received molecules at fully-absorbing RXs, we also consider molecular degradation in the environment.

Our major contributions are summarized as follows. We derive i) the exact closed-form expressions for the fraction of molecules absorbed, ii) the corresponding hitting rate, and iii) the asymptotic fraction of molecules absorbed as time approaches infinity at each RX with an impulse emission at the TX. Aided by a particle-based simulation method, we verify our analytical results. In addition, we present the distance ranges of two RXs that do not impact molecular absorption of each other. We also show that the mutual impact between two RXs reduces with the increase of degradation rate in the environment.

The rest of this paper is organized as follows. In Section II, we introduce the system model. In Section III, the closed-form expression for the fraction of absorbed molecules is derived. We also derive the corresponding hitting rate and the asymptotic fraction of absorbed molecules as time approaches infinity. In Section IV, we discuss the numerical results, and conclusion is presented in Section V.

II. System Model

In this letter, we consider a 1D unbounded environment where a single TX is located between two fully-absorbing RXs, i.e., RX_1 and RX_2, with distance d_1 from the RX_1 and distance d_2 from the RX_2, as depicted in Fig. 1. We consider the TX as a point source that can release an impulse of particles. We assume that the TX transmission starts at

X. Huang, N. Yang are with the Research School of Electrical, Energy and Materials Engineering, Australian National University, Canberra, ACT 2600, Australia (e-mail: {xinyu.huang1, nan.yang}@anu.edu.au).

Y. Fang is with the Department of Electrical and Electronic Engineering, University of Melbourne, Parkville, VIC 2010, Australia (e-mail: yuting.fang@unimelb.edu.au).

A. Noel is with the School of Engineering, University of Warwick, Coventry, CV 7AL, UK (e-mail: adam.noel@warwick.ac.uk).

This article has been accepted for publication in a future issue of this journal, but has not been fully edited. Content may change prior to final publication. Citation information: DOI 10.1109/LCOMM.2020.2981609, IEEE Communications Letters

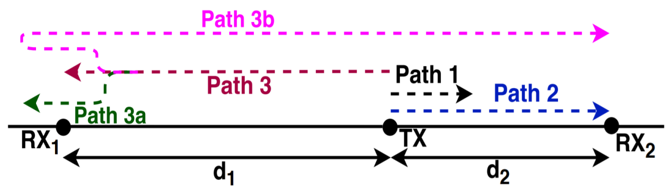

Fig. 1. Illustration of the system model, where one TX communicates with two fully-absorbing RXs in a one-dimensional environment.

$t = 0$ s. Once released, particles diffuse randomly with a constant diffusion coefficient D. We also consider the first-order chemical reaction (i.e., unimolecular degradation) in the environment, where type A molecules degrade into a new type of molecule ϕ that cannot be identified by the RXs, i.e., $A \xrightarrow{k} \phi$ [10, Ch. 9], where k $[\mathrm{s}^{-1}]$ is the degradation rate constant. We model the two RXs as point fully-absorbing RXs, which means that information molecules A are absorbed as soon as they hit the point RX_1 or RX_2.

III. Derivation of Channel Impulse Response

In this section, we derive closed-form expressions for the expected fraction of absorbed molecules at each RX for impulsive emission at the TX, and the asymptotic fraction of absorbed molecules at each RX as $t \to \infty$. We first derive the CR for impulsive emission when one RX exists, which builds the foundation for deriving the CR when two RXs exist. According to [11], the hitting rate for a single RX with molecular degradation can be obtained via the hitting rate without molecular degradation and multiplying by $\exp(-kt)$. Based on the existing expression for the hitting rate without molecular degradation in [6], the hitting rate at the RX at time t, denoted by $f(d,t)$, with molecular degradation is

$$f(d,t) = \frac{d}{\sqrt{4\pi D t^3}} \exp\left(-\frac{d^2}{4Dt} - kt\right), \tag{1}$$

where d is the distance between the TX and the RX. Using $\int_0^t f(d,u)\mathrm{d}u$, we obtain the fraction of molecules absorbed by time t, denoted by $F(d,t)$, as

$$F(d,t) = \frac{1}{2}\exp\left(-\sqrt{\frac{k}{D}}d\right)\mathrm{erfc}\left(\frac{d}{\sqrt{4Dt}} - \sqrt{kt}\right) + \frac{1}{2}\exp\left(\sqrt{\frac{k}{D}}d\right)\mathrm{erfc}\left(\frac{d}{\sqrt{4Dt}} + \sqrt{kt}\right). \tag{2}$$

As $t \to \infty$, we derive the asymptotic absorbed molecules $F(d, t\to\infty)$ as

$$F(d, t \to \infty) = \exp\left(-\sqrt{\frac{k}{D}}d\right). \tag{3}$$

In the following, we derive the CR when two RXs exist. We denote the fraction of absorbed molecules at RX_1 and RX_2 by time t for impulsive emission by $P_1(t)$ and $P_2(t)$, respectively. We also denote the corresponding hitting rates at RX_1 and RX_2 by $p_1(t)$ and $p_2(t)$, respectively.

To derive $p_1(t)$ and $p_2(t)$, we first discuss the impact of the existence of RX_1 on $p_2(t)$, based on [7]. As shown in Fig. 1, we classify all possible diffusion paths of molecules by time t in this environment into three paths, namely path 1, path 2, and path 3. Path 1 is for molecules diffusing in the environment, and path 2 and path 3 are for molecules that have hit RX_2 and RX_1, respectively. If only RX_2 exists, we can further classify path 3 into path 3a and path 3b. Path 3a represents molecules that do not hit RX_2 after firstly arriving at the location of RX_1 at time $\tau < t$, and path 3b represents molecules that hit RX_2 after firstly arriving at the location of RX_1 at time τ. Given that $f(d_2,t)$ denotes the hitting rate from the TX to RX_2 when only RX_2 exists, we find that $p_2(t)$ is less than $f(d_2,t)$, due to the existence of RX_1. Accordingly, $p_2(t)$ is obtained as [7, eq. (12)]

$$p_2(t) = f(d_2,t) - \gamma(t), \tag{4}$$

where $\gamma(t)$ is the reduced hitting rate impacted by the existence of RX_1. Based on the division in Fig. 1, $\gamma(t)$ is the hitting rate of path 3b and derived as

$$\gamma(t) = \int_0^t p_1(\tau) f(d_1+d_2, t-\tau)\mathrm{d}\tau, \tag{5}$$

where $f(d_1+d_2, t-\tau)$ is the hitting rate from RX_1 to RX_2 when RX_1 is regarded as the TX and RX_2 is the only RX. Combining (4) and (5), we derive $p_2(t)$ as [7, eq. (17)]

$$p_2(t) = f(d_2,t) - \int_0^t p_1(\tau) f(d_1+d_2, t-\tau)\mathrm{d}\tau. \tag{6}$$

Similarly, we obtain $p_1(t)$ as

$$p_1(t) = f(d_1,t) - \int_0^t p_2(\tau) f(d_1+d_2, t-\tau)\mathrm{d}\tau, \tag{7}$$

where $f(d_1,t)$ is the hitting rate from the TX to RX_1 when only RX_1 exists.

Based on (6) and (7), we solve the closed-form expressions for $P_2(t)$ and $p_2(t)$ in the following theorem:

Theorem 1: The fraction of absorbed molecules at RX_2 by time t for an impulsive emission of molecules is given by

$$\begin{aligned} P_2(t) = \sum_{i=0}^{\infty} [& R(2(i+1)d_1 + (2i+3)d_2, t, 2) \\ & - R(2(i+2)d_1 + (2i+3)d_2, t, 2) \\ & - R(2id_1 + (2i+1)d_2, t, 0) \\ & + R(2(i+1)d_1 + (2i+1)d_2, t, 0)], \end{aligned} \tag{8}$$

where $R(x,t,a)$ is given by

$$\begin{aligned} R(x,t,a) = & \frac{\theta}{2}\sqrt{\frac{k}{D}}\left(\alpha\beta(t) - \tilde{\alpha}\tilde{\beta}(t)\right) - \frac{i+1}{2}\Big(\tilde{\alpha}\tilde{\beta}(t) \\ & + \alpha\beta(t)\Big) - \frac{\theta}{\sqrt{\pi D t}}\exp\left(-\frac{x^2}{4Dt} - kt\right) \\ & + (i+1). \end{aligned} \tag{9}$$

In (9), $\theta = (d_1+d_2)(i+1)(i+a)$, $\alpha = \exp\left(x\sqrt{\frac{k}{D}}\right)$, $\tilde{\alpha} = \exp\left(-x\sqrt{\frac{k}{D}}\right)$, $\beta(t) = \mathrm{erfc}\left(\frac{x}{\sqrt{4Dt}} + \sqrt{kt}\right)$, and $\tilde{\beta}(t) = \mathrm{erfc}\left(\frac{x}{\sqrt{4Dt}} - \sqrt{kt}\right)$. The corresponding hitting rate at RX_2 by time t, $p_2(t)$, is obtained by taking the derivative of (8) with respect to t. By doing so, the expression for $p_2(t)$ is similar to (8), except for replacing $R(x,t,a)$ with $r(x,t,a)$, where $r(x,t,a) = \frac{\mathrm{d}R(x,t,a)}{\mathrm{d}t}$ and is given by

$$r\left(x,t,a\right) = \frac{i+1}{\sqrt{4\pi D t^3}} \exp\left(-\frac{x^2}{4Dt} - kt\right) \times \left(\left(1 - \frac{x^2}{2Dt}\right)\left(d_1+d_2\right)\left(i+a\right) - x\right). \quad (10)$$

Proof: Please see Appendix A. ∎

We denote the asymptotic fraction of absorbed molecules as $t \to \infty$ at RX_1 and RX_2 by $P_{1,\mathrm{asy}}$ and $P_{2,\mathrm{asy}}$, respectively. We derive and present $P_{2,\mathrm{asy}}$ in the following theorem:

Corollary 1: The asymptotic fraction of absorbed molecules at RX_2 as $t \to \infty$ is given by

$$P_{2,\mathrm{asy}} = \begin{cases} \frac{\exp\left(-d_2\sqrt{\frac{k}{D}}\right) - \exp\left(-(2d_1+d_2)\sqrt{\frac{k}{D}}\right)}{1-\exp\left(-2(d_1+d_2)\sqrt{\frac{k}{D}}\right)}, k \neq 0 \\ \frac{d_1}{d_1+d_2}, k = 0. \end{cases} \quad (11)$$

Proof: Please see Appendix B. ∎

Remark 1: The closed-form expressions for $P_1(t)$, $p_1(t)$ and $P_{1,\mathrm{asy}}$ are obtained by exchanging d_1 and d_2 therein for $P_2(t)$, $p_2(t)$ and $P_{2,\mathrm{asy}}$, respectively.

Remark 2: By setting $k=0$ in the expressions for $P_2(t)$ and $p_2(t)$, we can obtain the corresponding expressions without the occurrence of molecular degradation.

IV. Numerical Results

In this section, we present numerical results to validate our theoretical analysis in Section III and provide insightful discussions. The simulation results are conducted using a particle-based simulation method [12], where all results are averaged over 2000 realizations and the simulation time step is $\Delta t_{\mathrm{sim}} = 0.001$ s. Throughout this section, we set the diffusion coefficient $D = 79.4\ \mu\mathrm{m}^2/\mathrm{s}$ [13], an impulse of emission $N_{\mathrm{tx}} = 5000$ molecules, $\Delta t = 0.5$ s, and $k = 0.8\ \mathrm{s}^{-1}$, unless otherwise stated. In all figures, we observe precise agreement between our simulation results and the analytical curves generated from Section III, which demonstrate the validity of our analysis.

In Fig. 2, we investigate the number of summation terms that should be applied in (8). In Fig. 2(a), we apply three data sets to investigate the impact of d_1, d_2, and k on the number of summation terms. First, when only applying $i = \{0,1\}$ in (8), we observe that the equation first reaches the highest point, i.e., $P_{2,\mathrm{asy}}$, and then drops. Applying a larger number of terms results in $P_2(t) = P_{2,\mathrm{asy}}$ for a longer time, but increases computional complexity. To reduce such complexity, we clarify that applying $i = \{0,1\}$ is adequate since it enables (8) to reveal the absorbed molecules before becoming visually indistinguishable from the asymptotic value, and increasing terms in (8) does not change the absorbed molecules calculated before reaching the asymptotic value. After reaching the asymptotic value, we set $P_2(t) = P_{\mathrm{asy}}$. Second, comparing data set i) with data set ii) and data set iii), we observe that changing d_1, d_2, and k does not change the fact that applying $i = \{0,1\}$ is adequate for (8). In Fig. 2(b), we apply two data sets to investigate the impact of D on the number of terms.

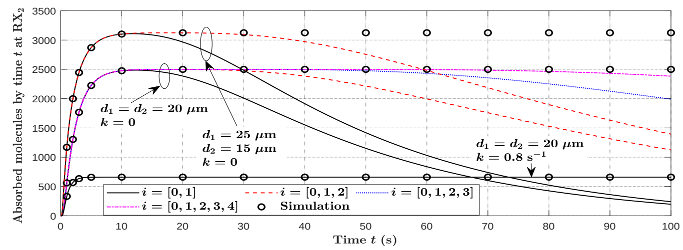

(a) Three data sets are applied: i) $d_1 = d_2 = 20\ \mu$m, $k = 0$, ii) $d_1 = 25\ \mu$m, $d_2 = 15\ \mu$m, $k = 0$, iii) $d_1 = d_2 = 20\ \mu$m, $k = 0.8\ \mathrm{s}^{-1}$, where $D = 79.4\ \mu\mathrm{m}^2/\mathrm{s}$ is applied for three data sets.

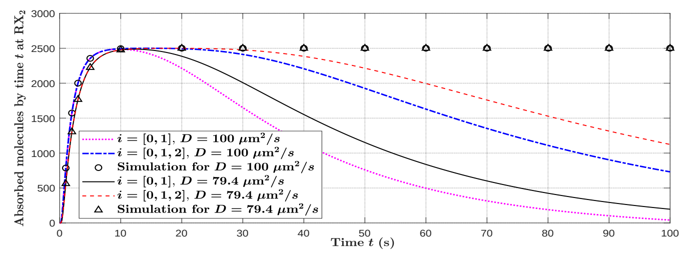

(b) Two data sets are applied: i) $d_1 = d_2 = 20\ \mu$m, $D = 79.4\ \mu\mathrm{m}^2/\mathrm{s}$, ii) $d_1 = d_2 = 20\ \mu$m, $D = 100\ \mu\mathrm{m}^2/\mathrm{s}$, where $k = 0$ is applied for two data sets.

Fig. 2. Absorbed molecules by time t at RX_2 versus time t, where different number of terms are applied in (8).

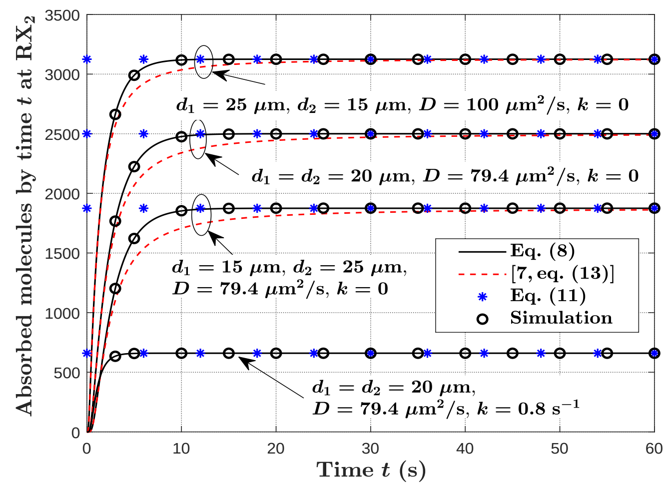

Fig. 3. Molecules absorbed by time t at RX_2 versus time t, where molecular emission is impulsive at the TX.

We still observe that changing D does not impact the fact that applying $i = \{0,1\}$ is adequate for (8).

In Fig. 3, we plot molecules absorbed at RX_2 by time t using (8) and [7, eq. (13)], respectively. We note that [7, eq. (13)] was initially applied to a 3D environment but can also be applied to a 1D environment[1]. In this figure, we first keep $k = 0\ \mathrm{s}^{-1}$ and vary d_1, d_2, and D to investigate the accuracy of (8) and [7, eq. (13)]. We also investigate the molecular degradation by setting $k = 0.8\ \mathrm{s}^{-1}$ and plot the absorbed

[1]In the 3D environment, [7] assumed that molecules are absorbed at the same points before reaching another RX. The points on RX_1 and RX_2 are denoted by s_1' and s_2', where s_1' and s_2' are found numerically. As RX_1 and RX_2 are regarded as points in a 1D environment, s_1' and s_2' are points RX_1 and RX_2. Substituting s_1' and s_2' with RX_1 and RX_2 in [7, eq. (13)], we obtain the fraction of absorbed molecules at RX_2 in a 1D environment, based on the method in [7].

This article has been accepted for publication in a future issue of this journal, but has not been fully edited. Content may change prior to final publication. Citation information: DOI 10.1109/LCOMM.2020.2981609, IEEE Communications Letters

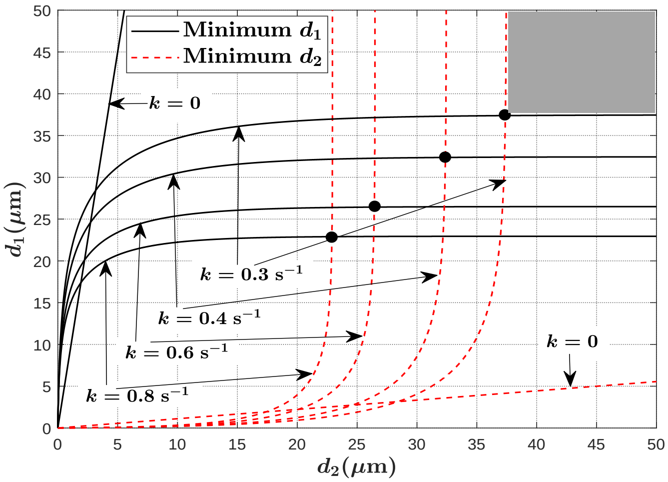

Fig. 4. Mimimum d_1 that does not influence absorbing molecules at RX$_2$ versus d_2, and minimum d_2 that does not influence absorbing molecules at RX$_1$ versus d_1, where different k is applied. Constraint for calculating minimum d_1 and minimum d_2 is 0.01, and the grey area represents distances of two RXs that do not impact each other when $k = 0.3$ s^{-1}.

molecules at RX$_2$ with (8). First, we clearly observe that the simulation matches well with (8) and a gap exists between the simulation and [7, eq. (13)] for 3 s $\leq t \leq$ 30 s, which demonstrates the accuracy advantage of (8) relative to [7, eq. (13)]. Second, we observe that the asymptotic value of (8) and [7, eq. (13)] converge as $t \to \infty$. Last, we observe that (11) matches with the simulation for both $k = 0$ and $k = 0.8$ s^{-1} when t is large, which demonstrates the correctness of (11).

In Fig. 4, we plot the minimum d_1 that does not impact molecular absorption at RX$_2$ versus d_2, and the minimum d_2 that does not impact molecular absorption at RX$_1$ versus d_1, for different k. We examine the impact of RX$_1$ on RX$_2$ based on the gap between the fraction of absorbed molecules at RX$_2$ and the fraction of absorbed molecules for the single RX as $t \to \infty$, which is expressed as $F(d_2, t \to \infty) - P_{2,\text{asy}}$, where $F(d_2, t \to \infty)$ is given by (3) and $P_{2,\text{asy}}$ is given by (11). We calculate the minimum d_1 which satisfies the condition $\left(F(d_2, t \to \infty) - P_{2,\text{asy}}\right)/F(d_2, t \to \infty) < 0.01$ for given d_2. We also suppose that RX$_1$ does not impact the molecular absorption at RX$_2$ when this condition is satisfied. Similarly, we calculate the minimum d_2 for given d_1. From this figure, we first observe that minimum d_1 intersects minimum d_2 when $k \neq 0$. The upper right area of the intersection for each k represents the range for d_1 and d_2 of two RXs that do not impact each other, because the condition for two RXs not impacting each other's molecular absorption is that d_1 and d_2 are simultaneously larger than minimum d_1 and minimum d_2, respectively. For example, if d_1 and d_2 are in the grey area, then two RXs do not impact each other when $k = 0.3$ s^{-1}. When $k = 0$, there is no intersection such that two RXs always impact each other. Second, we observe that the range for two RXs not impacting each other decreases with decreasing k. When k decreases, there is a larger number of molecules in the environment such that the mutual influence between two RXs is higher, which results in the less range for two RXs not impacting each other. Third, we observe that minimum d_1 and minimum d_2 firstly increase when d_2 and d_1 increase, respectively, and then become constant after the intersection. This is because increasing d_2 means that the molecular absorption at RX$_2$ decreases. In this case, if d_1 keeps the same value, then the molecular absorption at RX$_1$ relatively increases, which results in a larger impact on the molecular absorption at RX$_2$. Therefore, the minimum d_1 increases to reduce the impact on RX$_2$. Beyond the intersection, two RXs will not impact each other such that increasing d_2 will not lead to increase in minimum d_1.

V. Conclusion

In this letter, we focused on a 1D molecular communication system to investigate channel responses between a single TX and two fully-absorbing RXs. We derived new closed-form expressions for i) the fraction of absorbed molecules, ii) the corresponding hitting rate, and iii) the asymptotic fraction of absorbed molecules as time approaches infinity at each RX. Our results showed that our analytical expressions are accurate. We also investigated distance ranges for two RXs that do not impact molecular absorption of each other, which showed that the mutual influence between two RXs decreases with the increase in the degradation rate. Future work includes extending the 1D environment to 3D and deriving the CR between one TX and multiple RXs that partially absorb molecules.

Appendix A
Proof of Theorem 1

Taking the integral for both (6) and (7) over the interval $[0, t]$, we obtain

$$P_2(t) = F(d_2, t) - P_1(t) * f(d_1 + d_2, t), \tag{12}$$

$$P_1(t) = F(d_1, t) - P_2(t) * f(d_1 + d_2, t), \tag{13}$$

where $*$ is the convolution operator. Substituting $P_1(t)$ in (12) with (13) and performing the Laplace transform, we obtain

$$\mathcal{P}_2(s) = \frac{\exp\left(-d_2\sqrt{\frac{s+k}{D}}\right) - \exp\left(-(2d_1 + d_2)\sqrt{\frac{s+k}{D}}\right)}{s\left(1 - \exp\left(-2(d_1 + d_2)\sqrt{\frac{s+k}{D}}\right)\right)}, \tag{14}$$

where $\mathcal{P}_2(s)$ is the Laplace transform of $P_2(t)$. To obtain the inverse Laplace transform of (14), we define two new equations as

$$G(s) = \frac{\exp\left(-d_2\sqrt{\frac{s+k}{D}}\right) - \exp\left(-(2d_1 + d_2)\sqrt{\frac{s+k}{D}}\right)}{(s+k)\left(1 - \exp\left(-2(d_1 + d_2)\sqrt{\frac{s+k}{D}}\right)\right)} \tag{15}$$

and

$$H(s) = \underbrace{\frac{\exp\left(-\frac{d_2}{\sqrt{D}}s\right)}{s^2\left(1 - \exp\left(-\frac{2(d_1+d_2)}{\sqrt{D}}s\right)\right)}}_{H_1(s)} - \underbrace{\frac{\exp\left(-\frac{2(d_1+d_2)}{\sqrt{D}}s\right)}{s^2\left(1 - \exp\left(-\frac{2(d_1+d_2)}{\sqrt{D}}s\right)\right)}}_{H_2(s)}. \tag{16}$$

We note that $\mathcal{P}_2(s) = G(s) + \frac{k}{s}G(s)$ and $G(s) = H(\sqrt{s+k})$. Thus, we first solve the inverse Laplace transform of $H(s)$. From (16), we observe that $H_1(s)$ and $H_2(s)$ have similar forms. Thus, we only show the process of performing the inverse Laplace transform of $H_1(s)$. We re-write $H_1(s)$ as

$$H_1(s) = \exp\left(-\frac{d_2}{\sqrt{D}}s\right) \times \frac{1}{s\left(1-\exp\left(-\frac{d_1+d_2}{\sqrt{D}}s\right)\right)} \times \frac{1}{s\left(1+\exp\left(-\frac{d_1+d_2}{\sqrt{D}}s\right)\right)}. \tag{17}$$

According to [14, eqs. (5.1), (5.34), (5.36), (1.18)], the inverse Laplace transform of $H_1(s)$, denoted by $h_1(t)$, is

$$h_1(t) = \begin{cases} 0, \ 0 < t < \frac{d_2}{\sqrt{D}} \\ (i+1)\left(t - \frac{d_2}{\sqrt{D}} - \frac{d_1+d_2}{\sqrt{D}}i\right), \\ \frac{d_2}{\sqrt{D}} + \frac{2i(d_1+d_2)}{\sqrt{D}} < t < \frac{d_2}{\sqrt{D}} + 2(i+1)\frac{d_1+d_2}{\sqrt{D}}, \\ \qquad i = 0,1,2,3,... \end{cases} \tag{18}$$

According to [14, eq. (1.27)], the inverse Laplace transform of $H_1(\sqrt{s})$ is

$$\begin{aligned} \mathcal{L}^{-1}\left\{H_1(\sqrt{s})\right\} &= \frac{1}{2\sqrt{\pi t^3}}\int_0^\infty u\exp\left(-\frac{u^2}{4t}\right)h_1(u)\mathrm{d}u \\ &= \frac{1}{\sqrt{4\pi t}}\sum_{i=0}^{\infty}(i+1)\left[2\exp\left(-\frac{u^2}{4t}\right)\left(\frac{id_1+(i+1)d_2}{\sqrt{D}} - u\right)\right. \\ &\quad \left.\left. + \sqrt{4\pi t}\,\mathrm{erf}\left(\frac{u}{\sqrt{4t}}\right)\right]\right|_{\frac{2id_1+(2i+1)d_2}{\sqrt{D}}}^{\frac{2(i+1)d_1+(2i+3)d_2}{\sqrt{D}}}, \end{aligned} \tag{19}$$

where $F(x)\big|_a^b = F(b) - F(a)$. As aforementioned, $H_1(s)$ and $H_2(s)$ have similar forms. Therefore, the inverse Laplace transform of $H_2(\sqrt{s})$, denoted as $\mathcal{L}^{-1}\left\{H_2(\sqrt{s})\right\}$, can be derived analogously. Based on [14, eq. (1.3)], (19), and $\mathcal{L}^{-1}\left\{H_2(\sqrt{s})\right\}$, the inverse Laplace transform of $G(s)$, denoted by $g(t)$, is derived as

$$g(t) = \exp(-kt)\left(\mathcal{L}^{-1}\{H_1(\sqrt{s})\} - \mathcal{L}^{-1}\{H_2(\sqrt{s})\}\right). \tag{20}$$

Given $\mathcal{P}_2(s) = G(s) + \frac{k}{s}G(s)$, the inverse Laplace transform of $\mathcal{P}_2(s)$ is

$$P_2(t) = g(t) + k\int_0^t g(u)\mathrm{d}u. \tag{21}$$

Substituting (20) into (21), we obtain (8).

APPENDIX B
PROOF OF THEOREM 1

According to the final value theorem, if $P_2(t)$ has a finite limit as $t \to \infty$, we have

$$\lim_{t\to\infty} P_2(t) = \lim_{s\to 0} s\mathcal{P}_2(s). \tag{22}$$

When $k \neq 0$, substituting (14) into (22), we obtain

$$P_{2,\mathrm{asy}} = \frac{\exp\left(-d_2\sqrt{\frac{k}{D}}\right) - \exp\left(-(2d_1+d_2)\sqrt{\frac{k}{D}}\right)}{1-\exp\left(-2(d_1+d_2)\sqrt{\frac{k}{D}}\right)}. \tag{23}$$

When $k = 0$, we apply L'Hôpital's rule [15] to (23), and we have

$$\begin{aligned} P_{2,\mathrm{asy}} &= \lim_{k\to 0}\frac{\frac{\partial}{\partial k}\left(\exp\left(-d_2\sqrt{\frac{k}{D}}\right) - \exp\left(-(2d_1+d_2)\sqrt{\frac{k}{D}}\right)\right)}{\frac{\partial}{\partial k}\left(1-\exp\left(-2(d_1+d_2)\sqrt{\frac{k}{D}}\right)\right)} \\ &= \frac{d_1}{d_1+d_2}. \end{aligned} \tag{24}$$

Combining (23) and (24), we obtain (11).

REFERENCES

[1] T. Nakano, M. J. Moore, F. Wei, A. V. Vasilakos, and J. Shuai, "Molecular communication and networking: Opportunities and challenges," *IEEE Trans. Nanobiosci.*, vol. 11, no. 2, pp. 135–148, Jun. 2012.

[2] V. Jamali, A. Ahmadzadeh, W. Wicke, A. Noel, and R. Schober, "Channel modeling for diffusive molecular communication–a tutorial review," *Proc. IEEE*, Jun. 2019.

[3] N. Farsad, H. B. Yilmaz, A. Eckford, C.-B. Chae, and W. Guo, "A comprehensive survey of recent advancements in molecular communication," *IEEE Commun, Surveys Tuts.*, vol. 18, no. 3, pp. 1887–1919, Feb. 2016.

[4] Y. Fang, A. Noel, N. Yang, A. W. Eckford, and R. A. Kennedy, "Convex optimization of distributed cooperative detection in multi-receiver molecular communication," *IEEE Trans. Mol. Biol. Multi-Scale Commun.*, vol. 3, no. 3, pp. 166–182, Sep. 2017.

[5] Y. Lu, M. D. Higgins, A. Noel, M. S. Leeson, and Y. Chen, "The effect of two receivers on broadcast molecular communication systems," *IEEE Trans. Nanobiosci.*, vol. 15, no. 8, pp. 891–900, Oct. 2016.

[6] W. Guo, Y. Deng, B. Li, C. Zhao, and A. Nallanathan, "Eavesdropper localization in random walk channels," *IEEE Commun. Lett.*, vol. 20, no. 9, pp. 1776–1779, Sep. 2016.

[7] J. W. Kwak, H. Birkan Yilmaz, N. Farsad, C.-B. Chae, and A. Goldsmith, "Two-way molecular communications," pp. 1–11, Mar. 2019. [Online]. Available: arXiv: 1903.07865v2

[8] P. Cuatrecasas, "Membrane receptors," *Annu. Rev. Biochem.*, vol. 43, no. 1, pp. 169–214, Jul. 1974.

[9] R. D. Keynes, *Nerve and Muscle*. Cambridge, U.K.: Cambridge Univ. Press, 2001.

[10] R. Chang, *Physical Chemistry for the Biosciences*. University Science Books, 2005.

[11] A. C. Heren, H. B. Yilmaz, C.-B. Chae, and T. Tugcu, "Effect of degradation in molecular communication: Impairment or enhancement?" *IEEE Trans. Mol. Biol. Multi-Scale Commun.*, vol. 1, no. 2, pp. 217–229, Jun. 2015.

[12] S. S. Andrews and D. Bray, "Stochastic simulation of chemical reactions with spatial resolution and single molecule detail," *Phys. Biol.*, vol. 1, no. 3, p. 137, Aug. 2004.

[13] H. B. Yilmaz, A. C. Heren, T. Tugcu, and C.-B. Chae, "Three-dimensional channel characteristics for molecular communications with an absorbing receiver," *IEEE. Commun. Lett.*, vol. 18, no. 6, pp. 929–932, Jun. 2014.

[14] F. Oberhettinger and L. Badii, *Tables of Laplace Transforms*. Springer Science & Business Media, 1973.

[15] D. J. Struik, "The origin of L'Hôpital's rule," *The Math. Teach.*, vol. 56, no. 4, pp. 257–260, Apr. 1963.